Cell Reports, Volume *27*

Supplemental Information

In Situ Modification of Tissue Stem and Progenitor Cell Genomes

Jill M. Goldstein, Mohammadsharif Tabebordbar, Kexian Zhu, Leo D. Wang, Kathleen A. Messemer, Bryan Peacker, Sara Ashrafi Kakhki, Meryem Gonzalez-Celeiro, Yulia Shwartz, Jason K.W. Cheng, Ru Xiao, Trisha Barungi, Charles Albright, Ya-Chieh Hsu, Luk H. Vandenberghe, and Amy J. Wagers

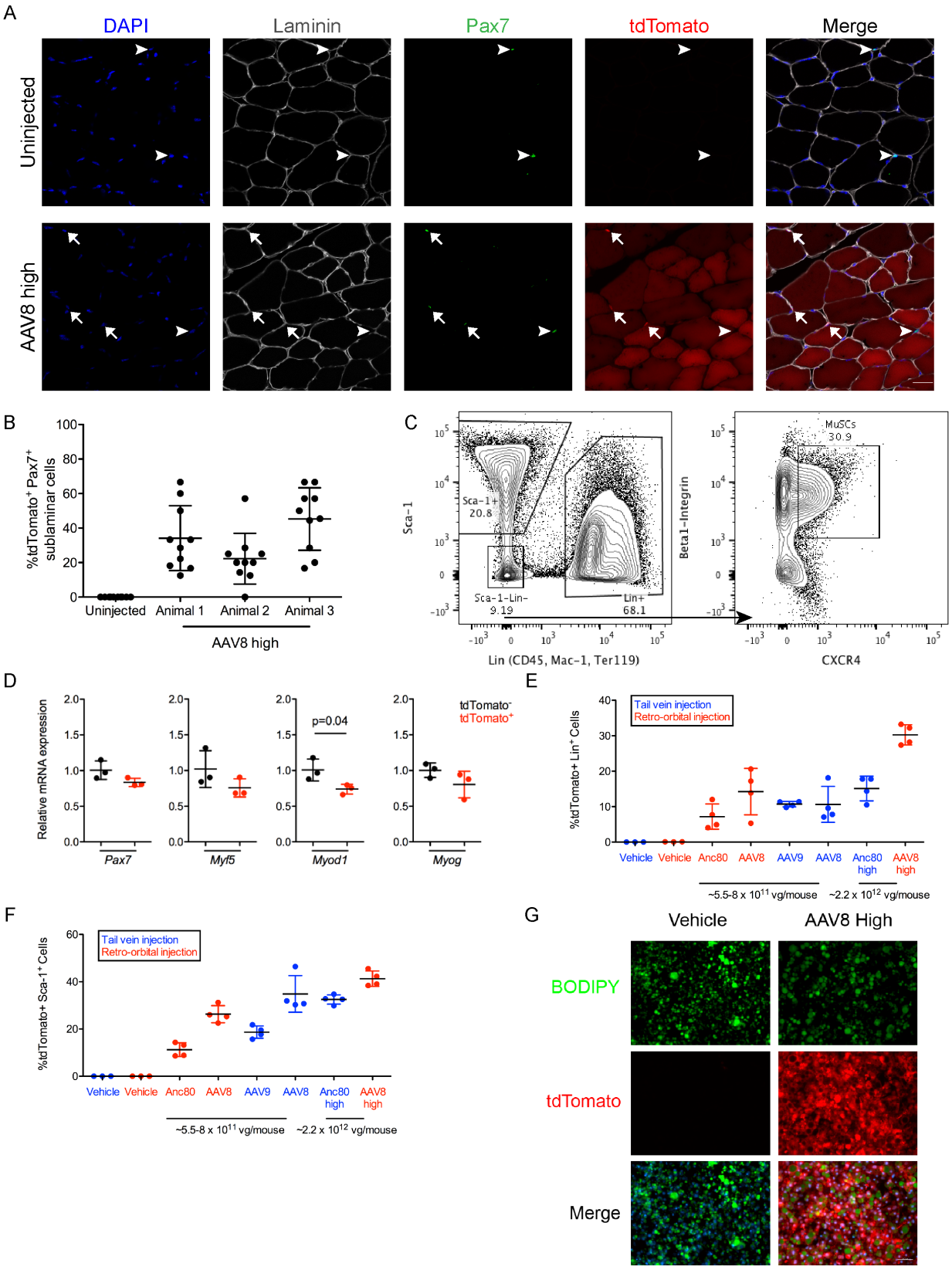
A
DAPI
Laminin
Pax7
tdTomato
Merge
Uninjected
AAV8 high
B
%tdTomato+ Pax7+ subliminar cells
Uninjected
Animal 1
Animal 2
Animal 3
AAV8 high
C
Sca-1
Lin (CD45, Mac-1, Ter119)
Sca-1+ 20.8
Sca-1-Lin- 9.19
Lin+ 68.1
Beta1-Integrin
CXCR4
MuSCs 30.9
D
Relative mRNA expression
Pax7
Myf5
Myod1
Myog
p=0.04
tdTomato-
tdTomato+
E
%tdTomato+ Lin+ Cells
Tail vein injection
Retro-orbital injection
Vehicle
Vehicle
Anc80
AAV8
AAV9
AAV8
Anc80 high
AAV8 high
~5.5-8 x 10^11 vg/mouse
~2.2 x 10^12 vg/mouse
F
%tdTomato+ Sca-1+ Cells
Tail vein injection
Retro-orbital injection
Vehicle
Vehicle
Anc80
AAV8
AAV9
AAV8
Anc80 high
AAV8 high
~5.5-8 x 10^11 vg/mouse
~2.2 x 10^12 vg/mouse
G
Vehicle
AAV8 High
BODIPY
tdTomato
Merge

Figure S1. Systemic injection of AAV-Cre transduces skeletal muscle satellite cells and mesenchymal progenitors.

Related to Figures 1 and 2

(A) Representative immunofluorescence images of tibialis anterior (TA) muscles collected from uninjected $Ai9^{fl/fl}$ mice (top) or from age-matched $Ai9^{fl/fl}$ mice 2 weeks after injection with high dose AAV8-Cre (bottom). n=4 injected mice analyzed. Scale bar, 20μm. (B) Quantification of the frequency of $tdTomato^+$ $Pax7^+$ satellite cells within TA muscles of uninjected or high dose AAV8-Cre injected $Ai9^{fl/fl}$ mice. n=1 uninjected mouse analyzed, n=3 high dose AAV8-Cre-injected mice analyzed; 60-80 $Pax7^+$ sublaminar cells were quantified among ten distinct $0.181mm^2$ fields per TA muscle. Individual data points are overlaid with mean ± SD. (C) *Left:* FACS gating strategy for Lin^+ ($CD45^+Mac\text{-}1^+Ter119^+$) hematopoietic cells and $Sca\text{-}1^+$ mesenchymal progenitors among myofiber-associated cells. *Right:* Gating strategy for $\beta1\text{-integrin}^+CXCR4^+$ MuSCs (muscle satellite cells) from the $Lin^-Sca\text{-}1^-$ parent gate using established cell surface markers (Cerletti et al., 2008; Maesner et al., 2016; Sherwood et al., 2004). (D) Real-time PCR analysis of *Pax7*, *Myf5*, *Myod1* and *Myog* expression in FACS-purified $tdTomato^+$ and $tdTomato^-$ satellite cells from mice injected with AAV8-Cre. *Gapdh* was used as a housekeeping gene. For each gene, transcript levels were normalized to the $tdTomato^-$ group. p-value calculated by paired t-test. (E, F) Quantification of AAV-transduced and Cre-recombined $tdTomato^+$ Lin^+ hematopoietic cells (E) and $Sca\text{-}1^+$ mesenchymal progenitors (F). Individual data points overlaid with mean ± SD. n=4 AAV-injected mice per group, n=3 vehicle-injected mice per group. (G) Representative fluorescence images of adipocytes differentiated *ex vivo* from $Sca\text{-}1^+$ mesenchymal progenitors isolated from mice injected with vehicle only (left column) or high dose AAV8-Cre (right column). Green, BODIPY (lipid stain). Red, tdTomato. Blue, Hoechst. Scale bar, 100μm. vg: viral genomes.

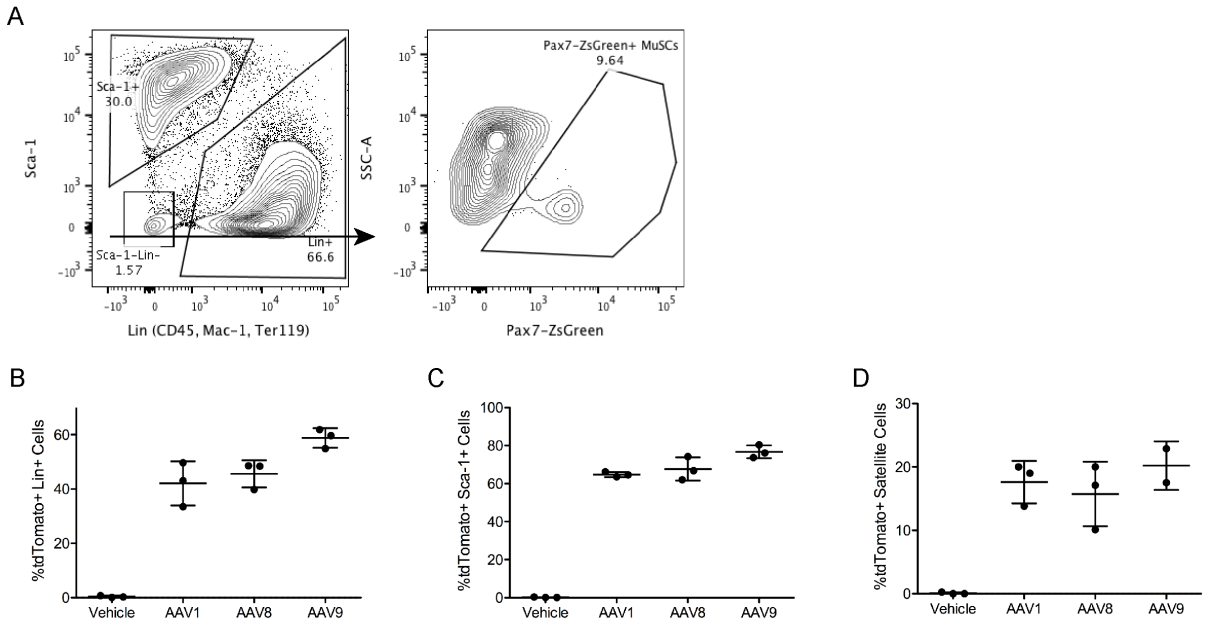

Figure S2. Local injection of AAV-Cre enables delivery to skeletal muscle satellite cells.
Related to Figures 1 and 2 and Table S1
(A) FACS gating strategy for Lin^+ ($CD45^+Mac\text{-}1^+Ter119^+$) hematopoietic cells, Sca-1^+ mesenchymal progenitors, and Sca-1^-Lin^-*Pax7-ZsGreen*$^+$ MuSCs (muscle satellite cells). Myofiber-associated cells were harvested from TA muscles of *Pax7-ZsGreen*$^{+/-}$;*mdx*;Ai9 mice injected with 6 x 10^{11} viral genomes (vg) of AAV-Cre. (B-D) Quantification of AAV-transduced and Cre-recombined $tdTomato^+$ Lin^+ hematopoietic cells (B), Sca-1^+ mesenchymal progenitors (C), and Sca-1^-Lin^-*Pax7-ZsGreen*$^+$ muscle satellite cells (D). Individual data points overlaid with mean ± SD. n=2-3 mice each group.

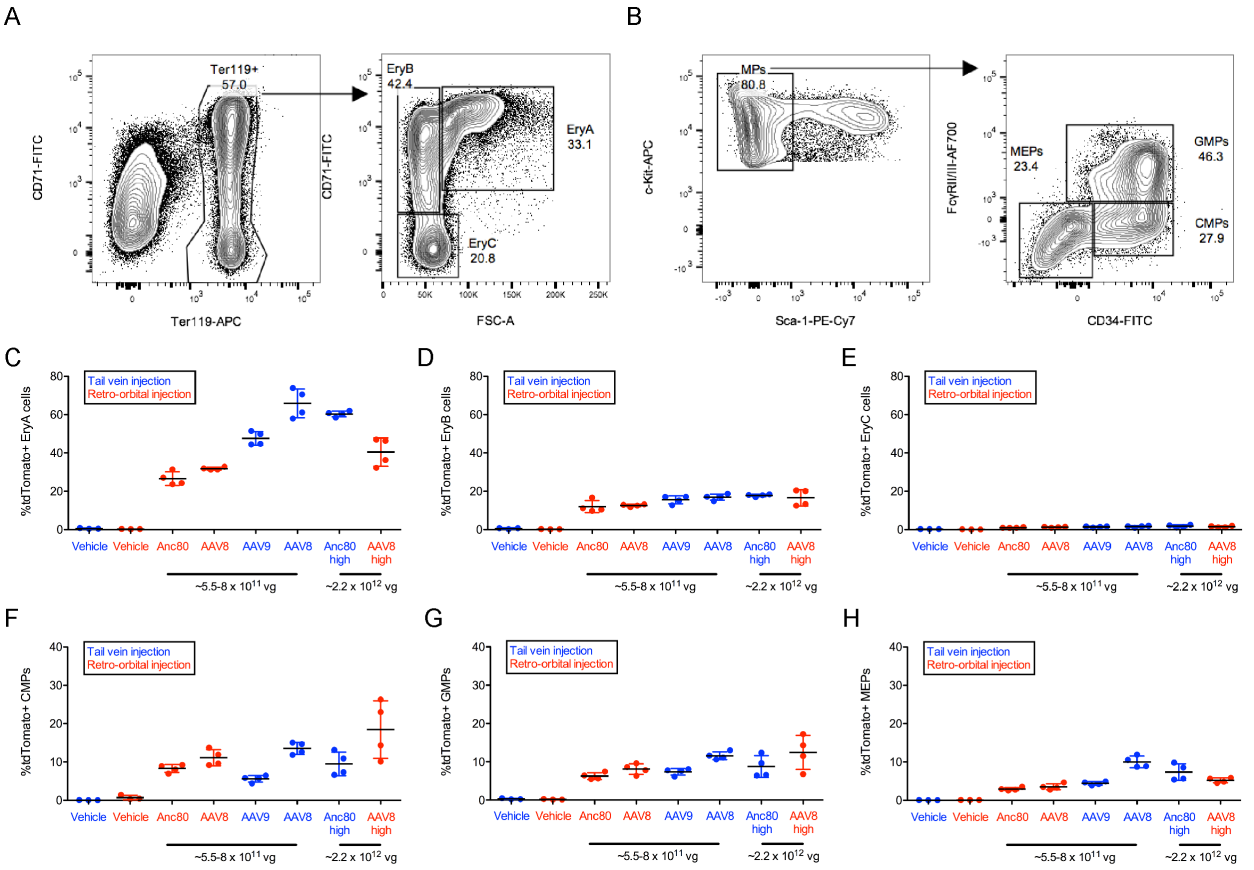

Figure S3. Systemic injection of AAV-Cre transduces hematopoietic progenitor cells.
Related to Figure 3

(A) FACS gating strategy for erythroid precursor cells: EryA ($Ter119^+CD71^+FSC^{high}$); EryB ($Ter119^+CD71^+ FSC^{low}$); and EryC ($Ter119^+CD71^-FSC^{low}$). Cells previously gated as live singlets. (B) FACS gating strategy for myeloid progenitor cells (MPs): Common Myeloid Progenitors (CMPs: $Lin^-Sca\text{-}1^-c\text{-}Kit^+CD34^+Fc\gamma R^{low}$); Granulocyte Monocyte Progenitors (GMPs: $Lin^-Sca\text{-}1^-c\text{-}Kit^+CD34^+Fc\gamma R^+$); and Megakaryocyte Erythroid Progenitors (MEPs: $Lin^-Sca\text{-}1^-c\text{-}Kit^+CD34^-Fc\gamma R^-$). MPs previously gated as $Lin^-c\text{-}Kit^+$ cells. (C-E) Frequency of (C) EryA, (D) EryB, and (E) EryC cells expressing tdTomato. Individual data points are overlaid with mean ± SD. n=4 AAV-injected mice per group, n=3 vehicle-injected mice per group. (F-H) Frequency of (F) CMPs, (G) GMPs and (H) MEPs expressing tdTomato. Individual data points are overlaid with mean ± SD. n=4 AAV-injected mice per group, n=3 vehicle-injected mice per group. Anc80L65 abbreviated Anc80. vg: viral genomes.

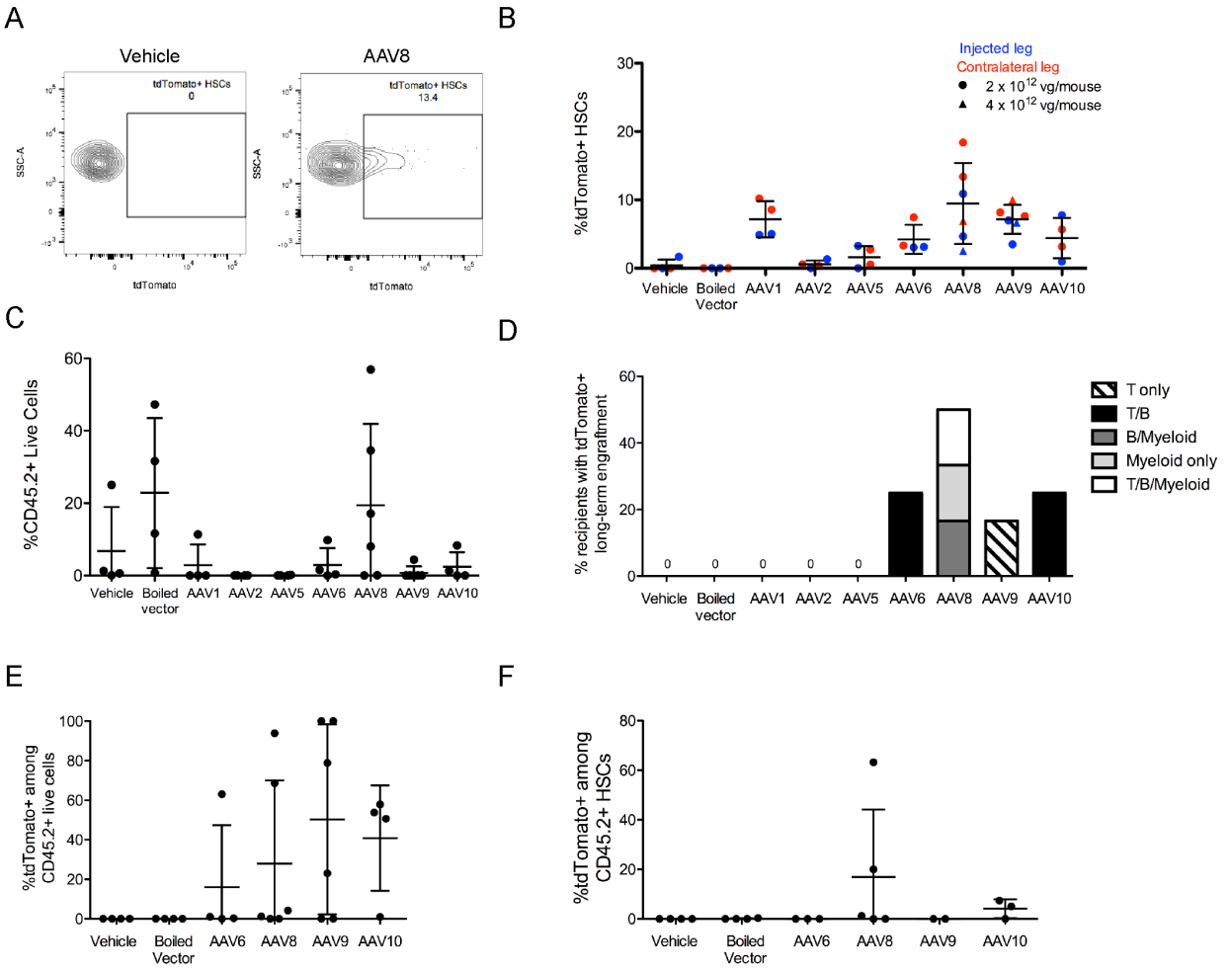

Figure S4. Local injection of AAV-Cre enables delivery to hematopoietic stem cells.
Related to Figure 3 and Table S2

(A) Representative flow cytometric analysis of tdTomato expression within HSCs 6 weeks after intrafemoral administration of AAV-Cre. (B) Frequency of $Lin^{-}Sca\text{-}1^{+}c\text{-}Kit^{+}CD48^{-}CD150^{+}$ HSCs expressing tdTomato within injected legs (blue) or contralateral legs (red). Individual data points are overlaid with mean ± SD. n=2-3 mice per serotype; injected and contralateral femurs were analyzed for each mouse. circles: mice injected with $2x10^{12}$ vg dose. triangles: mice injected with $4x10^{12}$ vg dose. The presence of $tdTomato^{+}$ HSCs in the contralateral leg reflects systemic dissemination of locally administered virus. (C) Percent donor chimerism among live peripheral blood cells in primary recipients at 16 weeks post transplantation. Individual data points are overlaid with mean ± SD. n=4-6 mice per group. (D) Frequency of primary recipients containing >1% $CD45.2^{+}$ cells and >1% $tdTomato^{+}$ among $CD45.2^{+}$ peripheral blood cells at 16 weeks post transplantation within indicated lineages. (E) Frequency of $tdTomato^{+}$ cells among live $CD45.2^{+}$ peripheral blood cells at 16 weeks post transplantation. Individual data points are overlaid with mean ± SD. n=4-6 mice per group. (F) Percentage of $tdTomato^{+}$ HSCs among donor-derived HSCs at 8 months post transplantation. Individual data points are overlaid with mean ± SD. n=2-5 mice per group. vg: viral genomes.

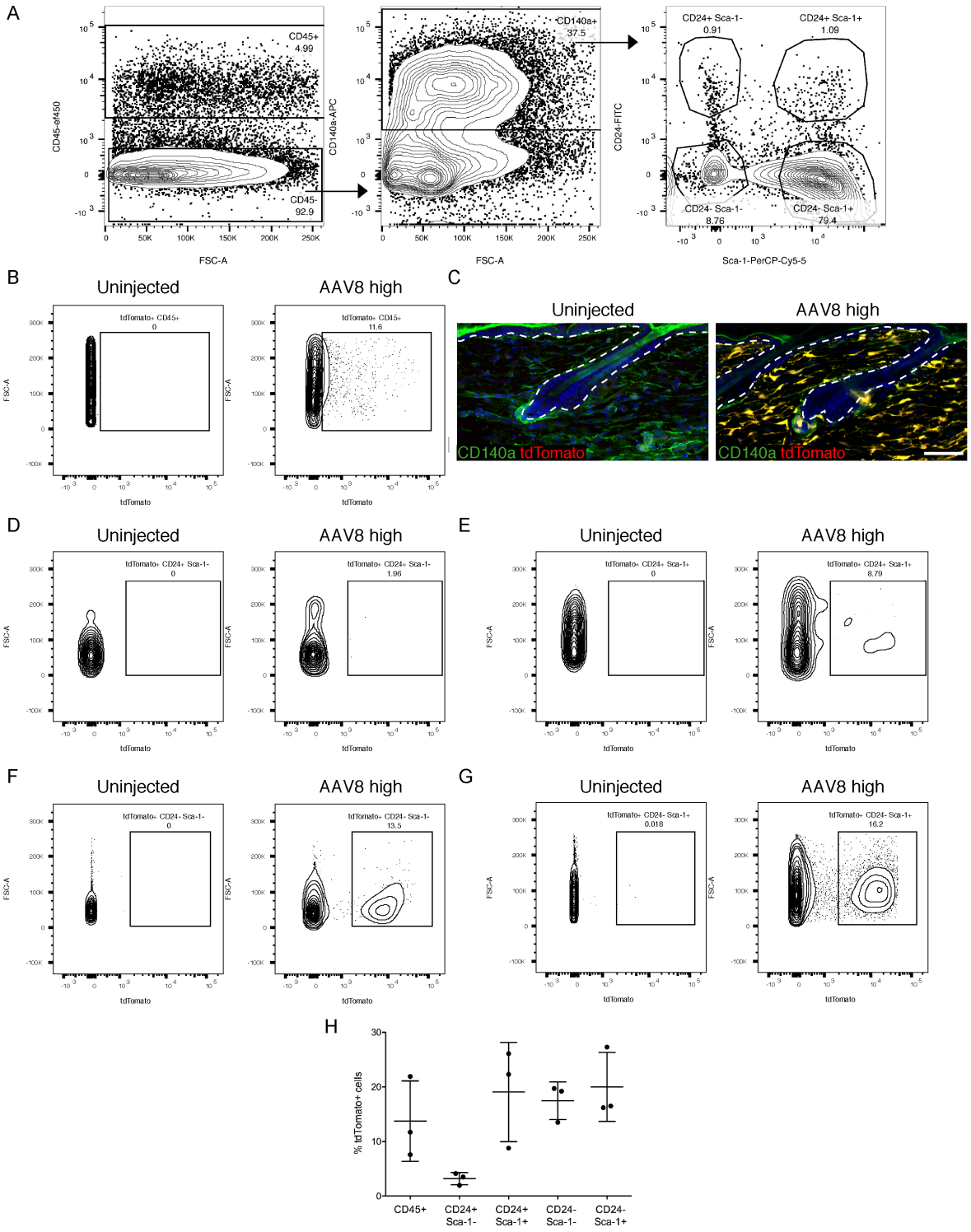

Figure S5. Systemic injection of AAV-Cre enables transduction of skin-resident hematopoietic cells, fibroblasts, and mesenchymal precursors.

Related to Figures 1-4

(A) Flow cytometry gating strategy to identify hematopoietic cells ($CD45^+$), dermal fibroblasts ($CD45^-CD140a^+$) and four subsets of dermal fibroblasts based on CD24 and Sca-1 expression within the skin dermis. Cells were previously

gated as live ($DAPI^-$) singlets. (B) Representative flow cytometric analysis of tdTomato fluorescence in $CD45^+$ cells from uninjected and high dose AAV8-Cre injected mice. (C) Representative immunofluorescence images of skin sections from uninjected and high dose AAV8-Cre injected mice. Green, CD140a. Red, tdTomato. Blue, DAPI. Scale bar, 50 μm. (D-G) Representative flow cytometric analysis of tdTomato fluorescence in (D) $CD24^+$ $Sca\text{-}1^-$ cells, (E) $CD24^+$ $Sca\text{-}1^+$ cells, (F) $CD24^-$ $Sca\text{-}1^-$ cells, and (G) $CD24^-$ $Sca\text{-}1^+$ cells. (H) Percentage of $tdTomato^+$ cells among each of the indicated skin cell populations from injected mice at 2 weeks post injection. Individual data points are overlaid with mean ± SD. n=3 AAV-Cre injected mice.

A

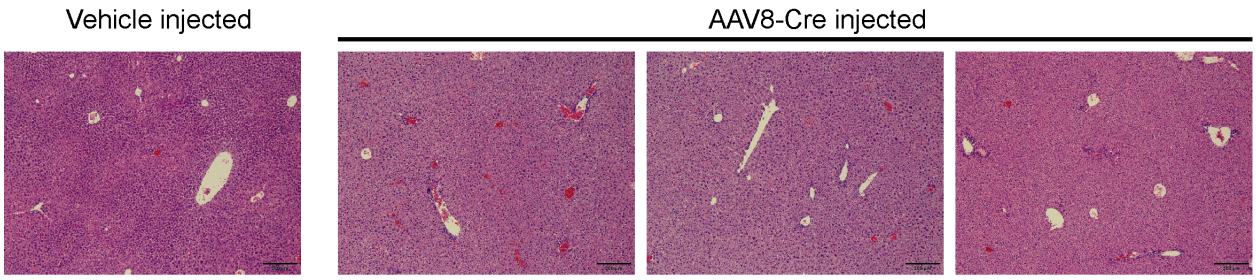

B

Condition	Dose	Liver Histopathology Scoring
AAV8-Cre	2 x 10^{12} vg	Normal (some microabscesses)
AAV8-Cre	2 x 10^{12} vg	Normal (some microabscesses)
AAV8-Cre	2 x 10^{12} vg	Slight increase in oval cells in portal areas
Vehicle	n/a	Small foci of necrosis
Uninjected WT	n/a	Normal (some microabscesses)

Figure S6. Systemic AAV administration does not induce overt liver histopathology.
Related to Figures 1-4
(A) Representative Hematoxylin and Eosin (H&E) images of liver sections from vehicle-injected or AAV8-Cre injected *mdx*;Ai9 animals. Injections performed intravenously. (B) Liver histopathology scoring from a subset of AAV8-Cre injected and vehicle-injected *mdx*;Ai9 mice, along with an uninjected C57BL/6J WT (wildtype) control. Tissues contained some microabscesses, which are common in normal mice, and small necrotic foci, which occur occasionally in normal mice. Scale bar, 200 μm. vg: viral genomes.

Table S1. Frequency of tdTomato$^+$ stem and progenitor cells in muscle and blood following systemic injections of AAV-Cre. Related to Figures 1-4.

	Muscle cells		Hematopoietic cells			
	%tdTomato$^+$ Satellite cells	%tdTomato$^+$ Sca-1$^+$ cells	%tdTomato$^+$ HSCs	%tdTomato$^+$ EryA cells	%tdTomato$^+$ EryB cells	%tdTomato$^+$ EryC cells
Condition	**Mean ± SD**	**Mean ± SD**	**Mean ± SD**	**Mean ± SD**	**Mean ± SD**	**Mean ± SD**
Vehicle (n=3 mice)	0.61 ± 0.695	0.47 ± 0.373	1.237 ± 0.225	1.327 ± 0.400	0.189 ± 0.129	0.002 ± 0.250
AAV6-Cre (4×10^{12} vg) (n=5 mice)	6.61 ± 0.847	5.25 ± 0.85	5.044 ± 1.111	4.514 ± 0.691	1.032 ± 0.403	0.250 ± 0.144
AAV8-Cre (4×10^{12} vg) (n=5 mice)	12.8 ± 1.991	6.16 ± 0.8	6.620 ± 2.236	7.772 ± 0.799	1.762 ± 0.124	0.432 ± 0.111
AAV9-Cre (4×10^{12} vg) (n=5 mice)	7.35 ± 1.669	5.41 ± 0.872	4.268 ± 0.712	5.842 ± 1.238	1.322 ± 0.238	0408 ± 0.122

Table S2.
Frequency of tdTomato$^+$ hematopoietic progenitor cells from local injections of AAV-Cre. Data were calculated by pooling the frequency of tdTomato$^+$ cells from the injected femurs and the contralateral femurs. Related to Figure 3.

	%tdTomato$^+$ Myeloid Progenitor cells (MPs)	%tdTomato$^+$ EryA cells	%tdTomato$^+$ EryB cells	%tdTomato$^+$ EryC cells
Condition	**Mean ± SD**	**Mean ± SD**	**Mean ± SD**	**Mean ± SD**
Vehicle (n=4 mice)	0.057 ± 0.040	1.425 ± 0.269	0.116 ± 0.039	0.005 ± 0.006
Boiled Vector (2×10^{12} vg) (n=4 mice)	0.039 ± 0.036	2.423 ± 0.449	0.112 ± 0.049	0.010 ± 0.012
AAV1-Cre (2×10^{12} vg) (n=4 mice)	19.398 ± 11.113	50.775 ± 13.007	16.350 ± 4.474	0.588 ± 0.168
AAV2-Cre (2×10^{12} vg) (n=4 mice)	0.702 ± 0.554	6.823 ± 3.820	0.818 ± 0.455	0.059 ± 0.049
AAV5-Cre (2×10^{12} vg) (n=4 mice)	1.013 ± 0.632	10.433 ± 3.097	1.853 ± 0.982	0.108 ± 0.068
AAV6-Cre (2×10^{12} vg) (n=4 mice)	28.670 ± 17.084	40.400 ± 14.073	7.778 ± 3.348	0.520 ± 0.192
AAV8-Cre (2×10^{12} vg) (n=4 mice)	40.825 ± 16.354	65.550 ± 21.579	18.078 ± 7.133	2.240 ± 1.280
AAV8-Cre (4×10^{12} vg) (n=2 mice)	14.130 ± 6.322	62.950 ± 9.970	20.150 ± 5.728	0.750 ± 0.255
AAV9-Cre (2×10^{12} vg) (n=4 mice)	30.000 ± 6.961	55.250 ± 7.703	11.173 ± 1.757	1.100 ± 0.446
AAV9-Cre (4×10^{12} vg) (n=2 mice)	26.600 ± 13.859	62.150 ± 17.607	18.550 ± 8.839	0.940 ± 0
AAV10-Cre (2×10^{12} vg) (n=4 mice)	26.310 ± 15.177	47.825 ± 22.849	10.278 ± 6.552	1.185 ± 0.998